AEDC-TR-73-60

A DESCRIPTION OF A PITCH/YAW DYNAMIC STABILITY, FORCED-OSCILLATION TEST MECHANISM FOR TESTING LIFTING CONFIGURATIONS

G. E. Burt

ARO, Inc.

June 1973

VON KÁRMÁN GAS DYNAMICS FACILITY
ARNOLD ENGINEERING DEVELOPMENT CENTER
AIR FORCE SYSTEMS COMMAND
ARNOLD AIR FORCE STATION, TENNESSEE

NOTICES

When U. S. Government drawings specifications, or other data are used for any purpose other than a definitely related Government procurement operation, the Government thereby incurs no responsibility nor any obligation whatsoever, and the fact that the Government may have formulated, furnished, or in any way supplied the said drawings, specifications, or other data, is not to be regarded by implication or otherwise, or in any manner licensing the holder or any other person or corporation, or conveying any rights or permission to manufacture, use, or sell any patented invention that may in any way be related thereto.

Qualified users may obtain copies of this report from the Defense Documentation Center.

References to named commercial products in this report are not to be considered in any sense as an endorsement of the product by the United States Air Force or the Government.

A DESCRIPTION OF A PITCH/YAW DYNAMIC STABILITY, FORCED-OSCILLATION TEST MECHANISM FOR TESTING LIFTING CONFIGURATIONS

G. E. Burt
ARO, Inc.

FOREWORD

The work reported herein was conducted by the Arnold Engineering Development Center (AEDC), Air Force Systems Command (AFSC), Arnold Air Force Station, Tennessee. The results were obtained by ARO, Inc. (a subsidiary of Sverdrup & Parcel and Associates, Inc.), contract operator of AEDC. The apparatus was developed under ARO Project No. VW5207. The wind tunnel tests were conducted on April 13, 1972, under ARO Project No. VT2233. The manuscript was submitted for publication on February 22, 1973.

This technical report has been reviewed and is approved.

ULES L. BARNWELL
Major, USAF
Research and Development Division
Directorate of Technology

ROBERT O. DIETZ
Director of Technology

ABSTRACT

A forced-oscillation test mechanism for measuring the dynamic stability derivatives in pitch or yaw on lifting configurations has been developed at AEDC-VKF. The mechanism will support models with a combined loading up to 1200-lb normal force and 300-lb axial force. Wind tunnel verification tests were conducted on AGARD Calibration Models B and C and Model B body alone at Mach numbers of 2.5, 3.0, 3.5, and 4.0 and at angles of attack from -4.5 to 11.5 deg. A description of the apparatus, testing technique, data reduction equations (including effects of sting bending), and the results from the laboratory bench and wind tunnel tests are included. The results of these tests were in good agreement with previous experimental data and theory.

CONTENTS

ILLUSTRATIONS

Figure

TABLE

NOMENCLATURE

A	Reference area, model wing planform area, 0.974 ft^2
b	Reference length for lateral coefficients, wing span, ft
C_m	Pitching-moment coefficient, pitching moment/$q_\infty Ac$
C_n	Yawing-moment coefficient, yawing moment/$q_\infty Ab$
C_{m_q}	Pitching-moment coefficient due to pitch velocity, $\partial(C_m)/\partial(qc/2V_\infty)$, $radian^{-1}$
$C_{m_{\dot{\alpha}}}$	Pitching-moment coefficient due to rate of change of angle of attack, $\partial(C_m)/\partial(\dot{\alpha}c/2V_\infty)$, $radian^{-1}$
C_{m_α}	Pitching-moment coefficient due to angle of attack, $\partial(C_m)/\partial\alpha$, $radian^{-1}$
C_{n_r}	Yawing-moment coefficient due to yaw velocity, $\partial(C_n)/\partial(rb/2V_\infty)$, $radian^{-1}$

C_{n_β}	Yawing-moment coefficient due to sideslip angle, $\partial(C_n)/\partial_\beta$, radian^{-1}
$C_{n_{\dot\beta}}$	Yawing-moment coefficient due to rate of change of sideslip angle, $\partial(C_n)/\partial(\dot\beta b/2V_\infty)$
c	Reference length for longitudinal coefficients, wing mean aerodynamic chord, 0.866 ft
I_y	Model moment of inertia about the cross-flexure pivot axis (y body axis), slug-ft^2
K_0	Cross flexure strain-gage-bridge calibration constant, radians/volt
K_1	Moment-beam strain-gage-bridge calibration constant, ft-lb/volt
K_s	Sting strain-gage-bridge calibration constant, ft-lb/volt
M	Aerodynamic pitching moment, ft-lb
M_b	Moment applied by the balance to oscillate the model, ft-lb
M_s	Moment applied to the sting as measured by the sting strain-gage bridge, ft-lb
M_p	Moment applied to the sting at the cross-flexure pivot, ft-lb
M_q	Pitching moment due to pitch velocity, $\partial M/\partial q$, ft-lb-sec/radian
M_α	Pitching moment due to angle of attack, $\partial M/\partial \alpha$, ft-lb/radian
$M_{\dot\alpha}$	Pitching moment due to rate of change of angle of attack, $\partial M/\partial\dot\alpha$, ft-lb-sec/radian
M_{θ_f}	Cross-flexure stiffness (with no static force loads unless otherwise specified), ft-lb/radian
δM_{θ_f}	M_{θ_f} (under load) - M_{θ_f} (no load), ft-lb/radian
$M_{\dot\theta_f}$	Cross-flexure damping moment, ft-lb-sec/radian
M_∞	Free-stream Mach number
p_o	Tunnel stilling chamber pressure, psia
q	Pitching velocity, radians/sec

q_∞	Tunnel free-stream dynamic pressure, lb/ft^2
r	Yawing velocity, radians/sec
$Re_{\infty, c}$	Tunnel free-stream Reynolds number based on c
T_o	Tunnel stilling chamber temperature, °R
t	Time, sec
V_∞	Tunnel free-stream velocity, ft/sec
W	Model mass, slugs
x_{cg}	Location of model center of gravity with respect to the pivot axis, ft
x_p	Location of the pivot axis with respect to the model nose, ft
z	Translation of the pivot axis normal to the sting (Fig. 5), ft
α	Angle of attack measured from the reference condition, α_M, radians
α_M	Mean angle of attack, deg
β	Sideslip angle, radians
Γ	Phase angle between sting oscillation angle, θ_s, and flexure oscillation angle, θ_f (positive when θ_s leads), radians or deg
γ	Phase angle between input moment, M_b, and flexure oscillation angle, θ_f (positive when M_b leads), radians or deg
θ	Angular displacement in pitch, radians
ω	Model angular oscillation frequency, radians/sec
ω_{n_f}	Model-flexure natural frequency at vacuum conditions $(= \sqrt{-M_{\theta_f}/I_y})$, radians/sec
ω_{n_s}	Natural frequency of the model-sting system, radians/sec
$(\dot{}), (\ddot{})$	First and second derivatives with respect to time, t
$(\bar{})$	Amplitude
$\Delta( )$	Probable error

SUBSCRIPTS

f	Cross flexure
m	Model
mag	Magnetic calibrator
S	Static component
s	Sting

SECTION I
INTRODUCTION

The advent of high performance, supersonic, military airplanes and lifting reentry bodies such as the F-15, B-1, and space shuttle has created the requirement to develop new dynamic stability test mechanisms for the AEDC von Kármán Gas Dynamics Facility (VKF) continuous flow wind tunnels. To meet the requirements for large lift loads, relatively large damping moments, and to maintain compatibility with expected model configurations, the forced-oscillation technique was selected. This is a proven technique currently being used at the VKF for measuring damping coefficients due to pitch and yaw rate on configurations with relatively small lift forces (Ref. 1). This report covers the development and checkout, including wind tunnel verification testing, of a mechanism to measure these coefficients on lifting configurations. This mechanism can support models with a combined loading up to 1200-lb normal force and 300-lb axial force. These large lift forces, when combined with slender stings required for testing airplane configurations, can create sting oscillations that must be accounted for in the data reduction equations.

The mechanism was designed primarily for use in the VKF supersonic and hypersonic wind tunnels (Mach 1.5 to 10) but can be used in the Propulsion Wind Tunnel Facility (PWT) transonic and supersonic tunnels (Mach 0.2 to 4.75). The wind tunnel verification tests were conducted in the VKF Supersonic Wind Tunnel (A) at Mach numbers from 2.5 to 4.0 on AGARD Calibration Models B and C and on Model B with the wings removed.

A test mechanism to measure the dynamic stability derivatives in roll on lifting configurations has also recently been developed at AEDC-VKF, Ref. 2. A description of the testing technique, apparatus, and verification wind tunnel test results obtained on the AGARD Calibration Model B is reported in Ref. 2.

SECTION II
APPARATUS

2.1 TEST MECHANISM

The pitch/yaw damping test mechanism (VKF 1. B) shown in Fig. 1 utilizes a cross-flexure pivot, a one-component moment beam, and an electric shaker motor. The motor is coupled to the moment beam by means of a connecting rod and flexural linkage which converts the translational force to a moment (70-in.-lb maximum) to oscillate the model at amplitudes up to ±2 deg and frequencies from 2 to 20 Hz. The cross flexures, which are instrumented to measure the pitch/yaw displacement, support the model loads and provide the restoring moment to cancel the inertia moment when the system is operating at its natural frequency. The existing cross flexures are composed of three 0. 170-in.-thick beams with single unit construction and produce a restoring moment of -938 ft-lb/radian. Additional cross-flexure units can be fabricated with different thicknesses to produce restoring moments from -50 to -1700 ft-lb/rad and still support the required loads and allow for ±2-deg deflection. Since the moment beam which is used to measure the forcing moment is not subjected to the static loads, it can be made as sensitive as required for the dynamic measurements. Presently, two beams exist which can measure up to ±25 and ±70 in.-lb. A pneumatic- and spring-operated locking device is provided to hold the model during injection into or retraction from the tunnel or during tunnel starts. The sting cross section is elliptical (Fig. 1a) to optimize strength and clearance for oscillating slender models. It is not water cooled, but it is interchangeable with the 1. 75-in.-diam, water-cooled sting for the roll dynamic stability mechanism (Ref. 2) which permits tests to be conducted in the hypersonic tunnels. The water-cooled sting is 6. 1 in. shorter than the elliptical sting.

2.2 INSTRUMENTATION

The forced-oscillation instrumentation described in Ref. 1 was modified to produce better control and monitor systems and more accurate data with less computer time required. These changes were made possible by using an electronic analog system with precision electronics. The control, monitor, and data acquisition instrumentation are contained in a portable console (Fig. 2) that can be easily interfaced with the instrumentation of the various wind tunnels. The same basic instrumentation system is used for the forced-oscillation, roll test mechanism (Ref. 2).

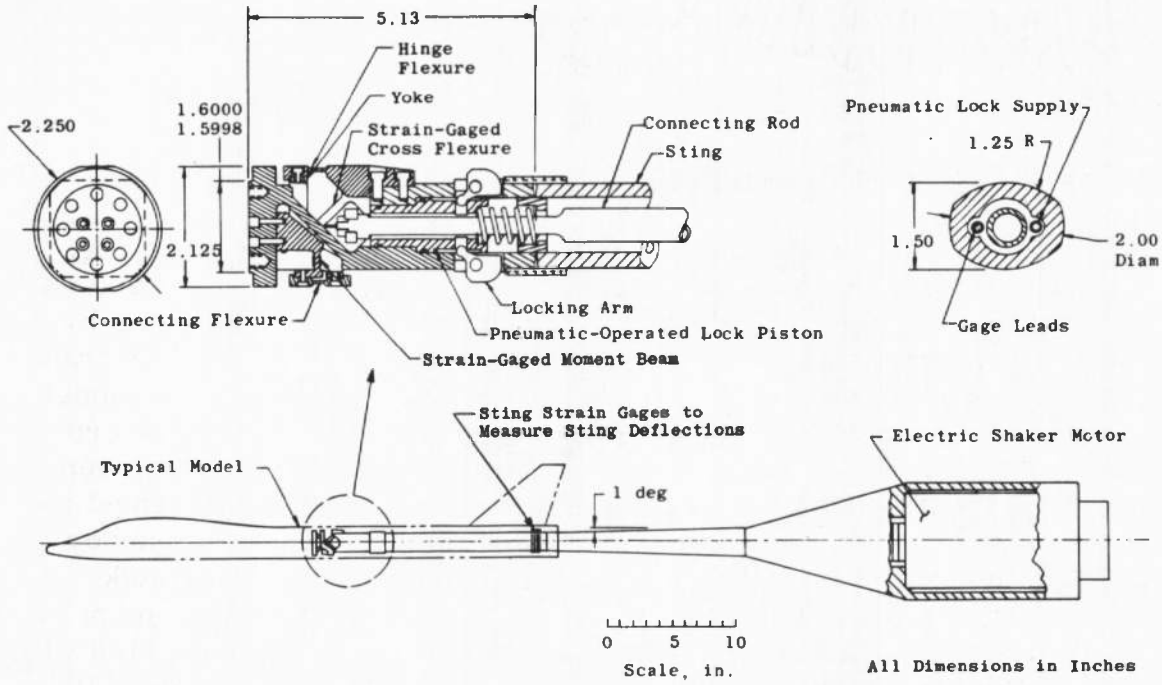

a. Details

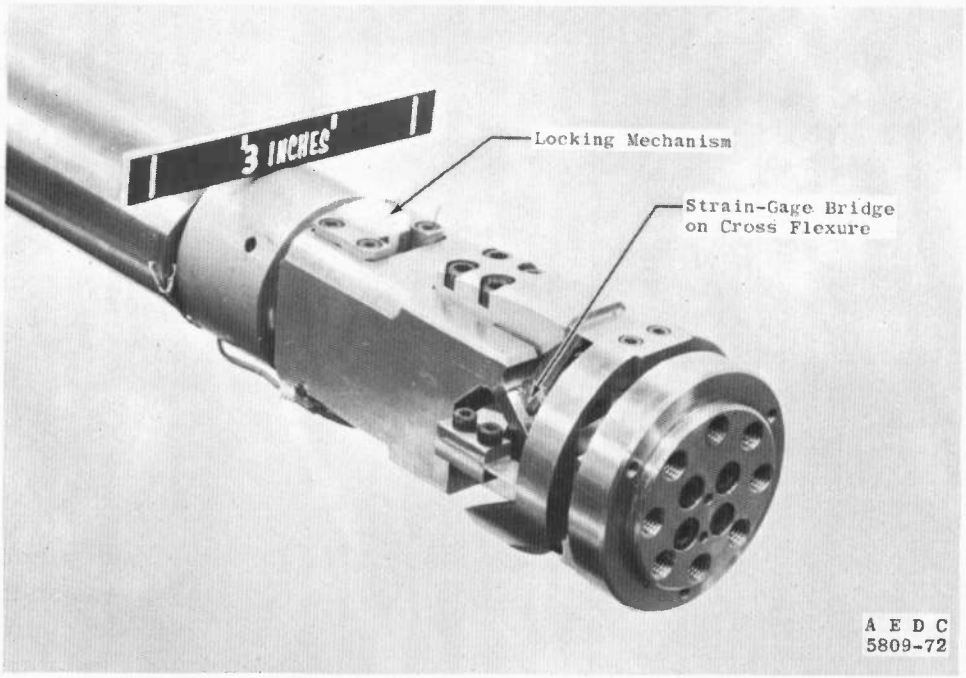

b. Photograph of the Balance Assembly

Fig. 1 VKF 1.B Test Mechanism

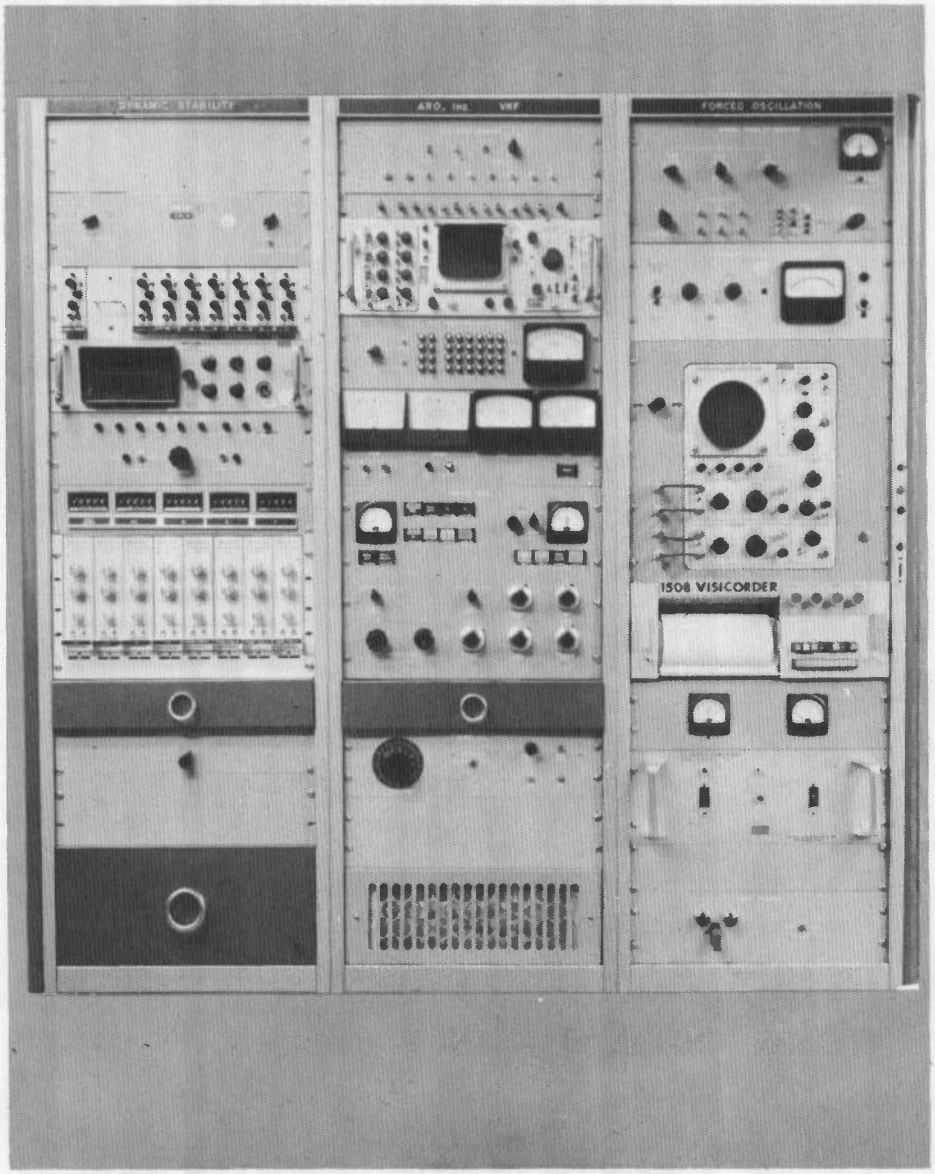

Fig. 2 Instrumentation Console

The control instrumentation provides a system which can vary the oscillation frequency, oscillation amplitude, and position of the model within the flexure and balance limits. An electronic feedback loop is used to control the oscillation amplitude which permits testing both dynamically stable and unstable configurations.

Data are normally obtained at or near the natural frequency of the model-flexure system; however, electronic resolvers permit data to be

obtained off resonance. A schematic of the data acquisition system is shown in Fig. 3. The gages on the flexures, balance, and sting are excited by d-c voltages, and outputs are increased to optimum values by d-c amplifiers. Typical outputs from an oscillating model are composed of oscillatory components (OC) superimposed on static components (SC). These components are separated in the data system by bandpass and lowpass filters. The SC outputs are sent directly through the tunnel scanner to the computer which calculates the static pitching-moment coefficient, C_m, and sting deflections. The OC outputs are input to the resolver instrumentation (Fig. 3b) and precise frequency measuring instrumentation which was developed at the VKF. The resolvers process the OC signals and output d-c voltages which are proportional to the amplitude squared, the in-phase and quadrature (90 deg out of phase) balance components, and the in-phase and quadrature sting components. The resolver and frequency instrument outputs are input to the tunnel scanner and sent to the computer which reduces the data to the aerodynamic coefficients, $C_{m_q} + C_{m_{\dot{\alpha}}}$ and C_{m_α}, as discussed in Section 3.1. The frequency instrument controls the length of the data interval in increments from approximately 2 to 25 sec during which the scanner reads each input approximately ten times per second.

2.3 MODELS

The three models used for the wind tunnel verification tests included an AGARD Calibration Model B, an AGARD Calibration Model C which was made by adding a tail assembly to the Model B (Fig. 4), and the Model B without wings. These models were furnished by the Cornell Aeronautical Laboratory. The body is a tangent ogive-cylinder (4.5-in.-diam) with a fineness ratio of 8.5. The 60-deg delta wing has a symmetrical circular-arc cross section with a thickness ratio of 0.04 and a span of four body diameters. The tail assembly for the Model C consists of a cylindrical body that is 1.5 body diameters long on which is mounted a T tail. The horizontal tail is a 60-deg delta which is located 1.42 body diameters above the body centerline and has a span of 1.63 diameters. The vertical tail is swept 60 deg and tapered to produce a trailing-edge angle of 45 deg. The cross section of the horizontal and vertical tails is also a symmetrical circular arc with a thickness ratio of 0.04. The model body was constructed of aluminum with a steel section at the wing mounting location. The wings were aluminum, and the tail assembly for Model C was steel. The model was mounted to the test mechanism such that there were 3.1 body diameters from the model base to the sting flare for Model C.

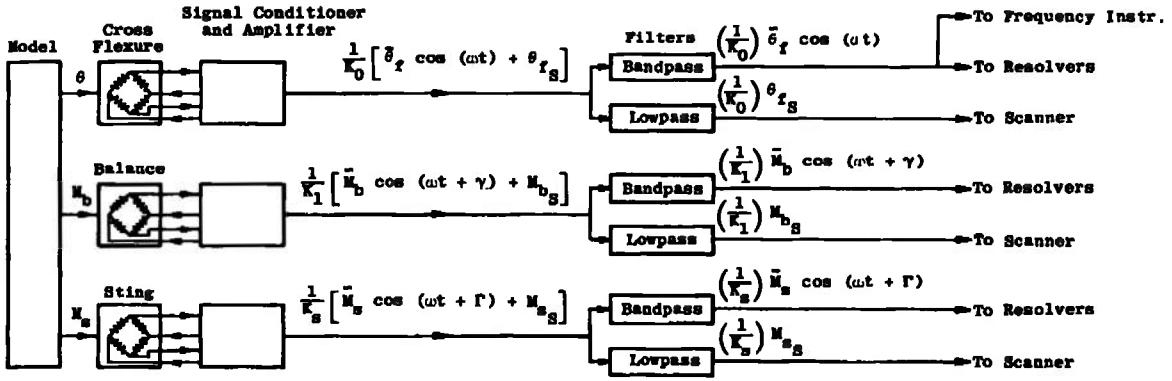

a. Basic Outputs

Fig. 3 Data Acquisition Instrumentation Schematic

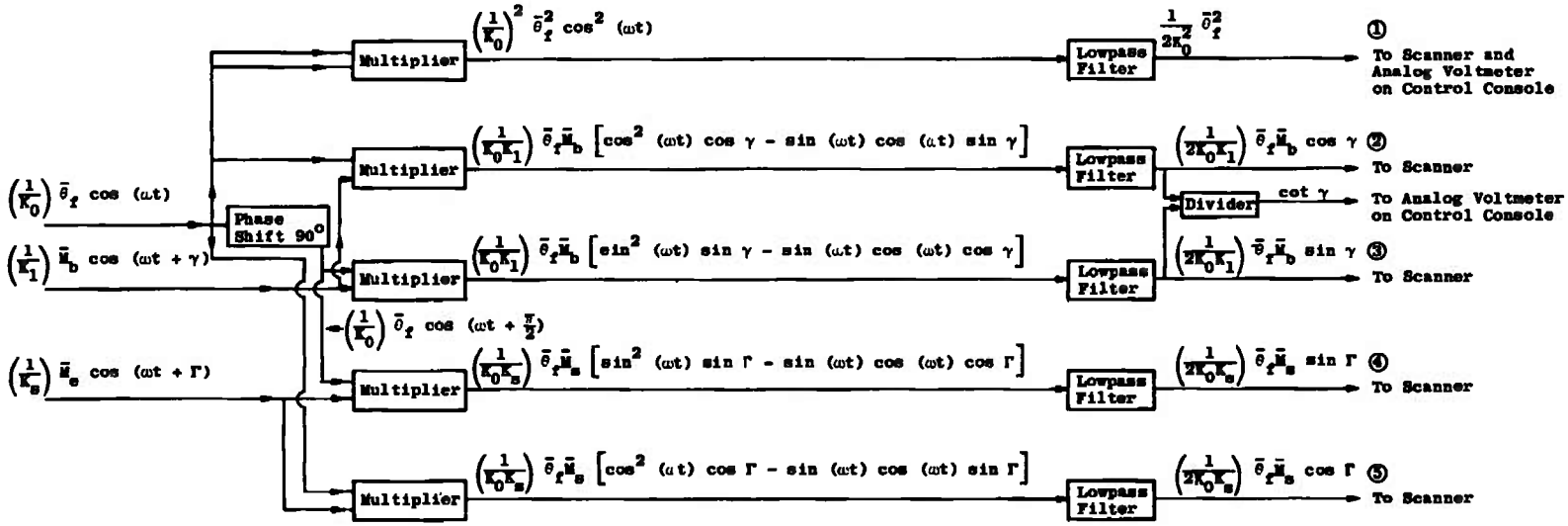

b. Resolver System

Fig. 3 Concluded

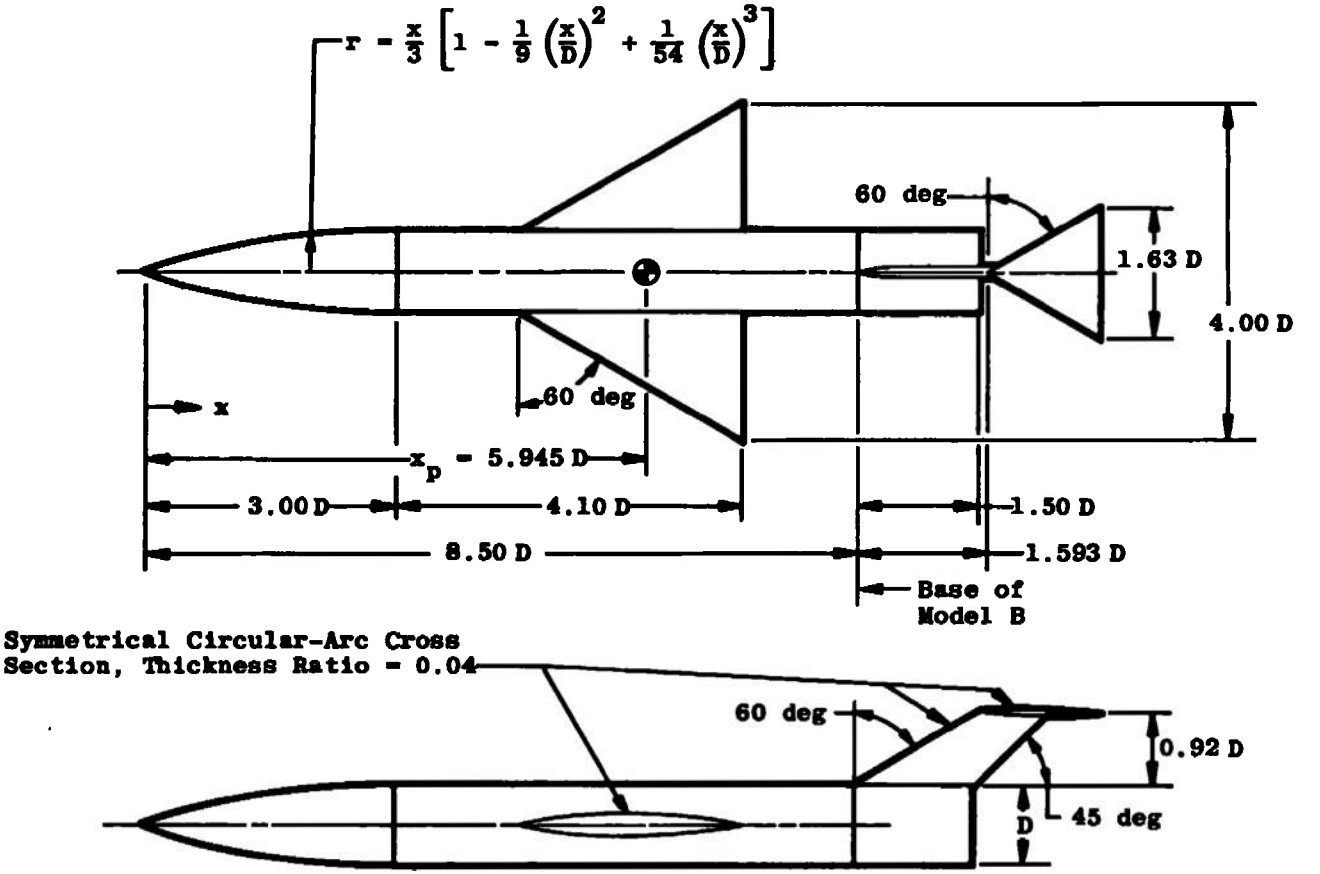

Notes: AGARD Calibration Model C Shown
All Dimensions Are in Body Diameters, D
D = 4.50 in.

● Indicates Pivot Axis and Moment Reference Point

a. Details

Fig. 4 Model Description

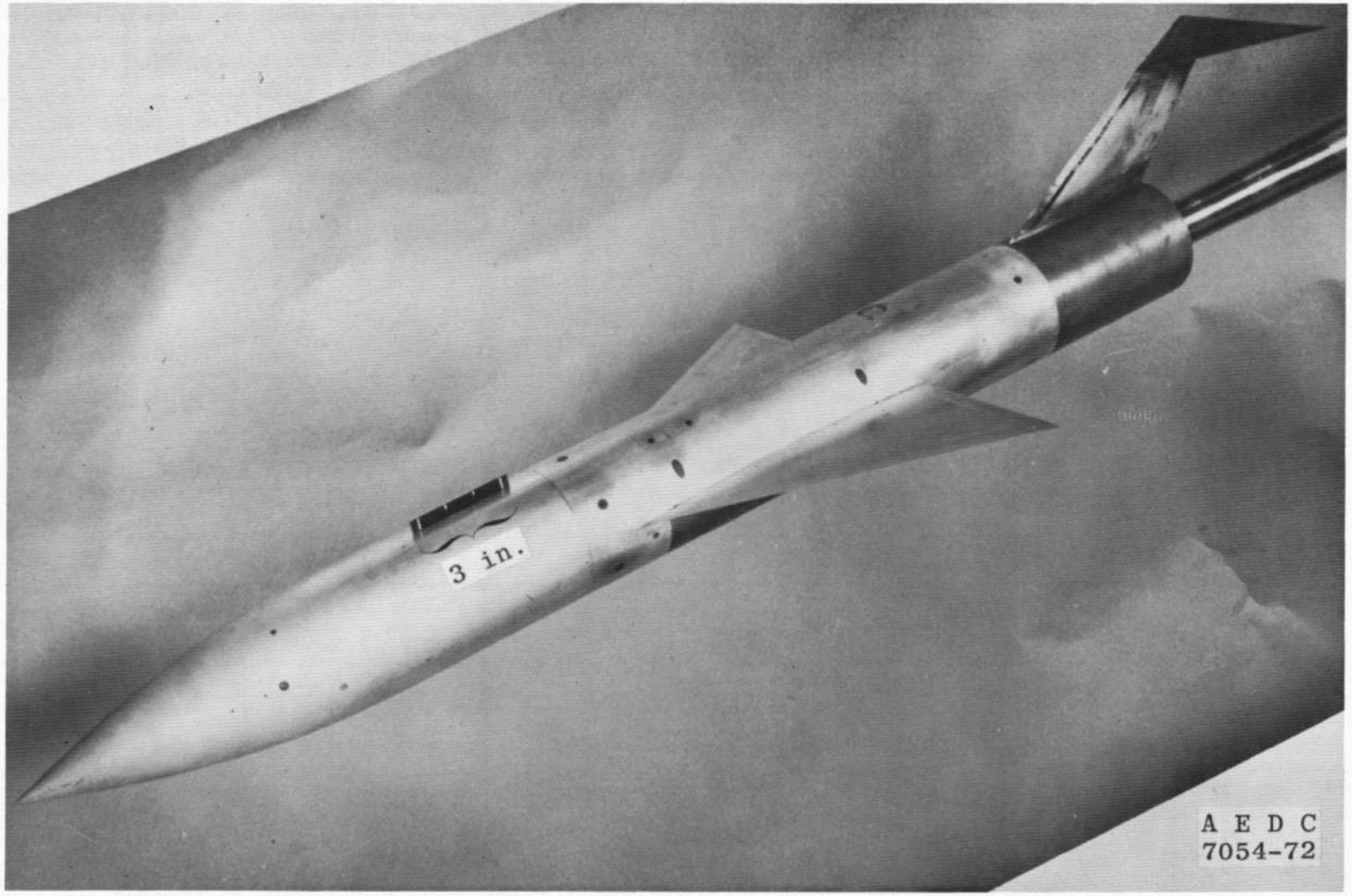

b. Installation Photograph of AGARD Calibration Model C
Fig. 4 Concluded

2.4 WIND TUNNEL

Tunnel A is a continuous, closed-circuit, variable density wind tunnel with an automatically driven flexible-plate-type nozzle and a 40- by 40-in. test section. The tunnel can be operated at Mach numbers from 1.5 to 6 at maximum stagnation pressures from 29 to 200 psia, respectively, and stagnation temperatures up to 750°R ($M_\infty = 6$). Minimum operating pressures range from about one-tenth to one-twentieth of the maximum at each Mach number. Mach number changes may be made without stopping the tunnel in most instances. The model can be injected into the tunnel for a test run and then retracted for model changes without stopping the tunnel flow.

SECTION III
PROCEDURE

3.1 DATA REDUCTION

The test mechanism was intended to operate as a one-degree-of-freedom system in pitch or yaw; but since the sting had to be slender to test aircraft configurations which transmit relatively large oscillatory normal forces to the sting as the model oscillates in pitch, the system had to be analyzed as a two-degree-of-freedom system. Figure 5 shows a schematic of a model oscillating in pitch about the cross-flexure pivot and translating normal to the sting. It should be noted that as the mechanism is pitched, static forces and moments are applied which deflect the sting and balance. These static deflections affect only the mean angle of attack, α_M, and for clarity are not shown in Fig. 5. The moment equation-of-motion of the system shown in Fig. 5, written in body axis about the cross-flexure pivot and allowing for model unbalance (normally models are balanced before testing, but some slender configurations cannot be accurately balanced), is

$$I_y\ddot{\theta}_m - Wx_{cg}\ddot{z} - M_q\dot{\theta}_m - M_{\dot{\alpha}}\dot{\alpha} - M_{\dot{\theta}_f}\dot{\theta}_f - M_\alpha\alpha - \left(M_{\theta_f} + \delta M_{\theta_f}\right)\theta_f = M_b \qquad (1)$$

The δM_{θ_f} term is included because the flexure stiffness varies (slightly for the existing flexures) with axial and normal force (Ref. 3). δM_{θ_f} is determined in the data reduction from known or estimated force data. Bench tests have shown that $M_{\dot{\theta}_f}$ is essentially unaffected by static loads.

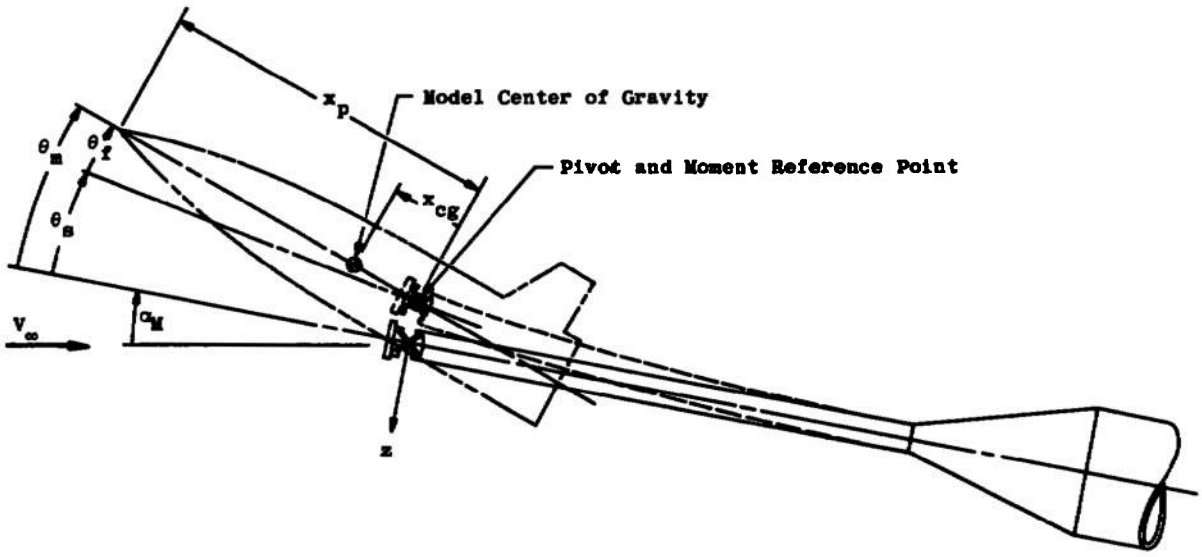

Fig. 5 Schematic Illustrating Model and Bent-Sting Orientation

The measured displacements with this system are the flexure rotation, θ_f, and the sting deflections, θ_S and z. From Fig. 5 the following identities can be obtained:

$$\theta_m = \theta_f + \theta_s \tag{2}$$

$$\alpha = \theta_m + \frac{\dot{z}}{V_\infty \cos \alpha_M} \tag{3}$$

Substituting in Eq. (1) gives:

$$I_y(\ddot{\theta}_f + \ddot{\theta}_s) - Wx_{cg}\ddot{z} - M_q(\dot{\theta}_f + \dot{\theta}_s) - M_{\dot{\alpha}}\left(\dot{\theta}_f + \dot{\theta}_s + \frac{\ddot{z}}{V_\infty \cos \alpha_M}\right) - M_{\dot{\theta}_f}\dot{\theta}_f - M_\alpha\left(\theta_f + \theta_s + \frac{\dot{z}}{V_\infty \cos \alpha_M}\right)$$

$$- \left(M_{\theta_f} + \delta M_{\theta_f}\right)\theta_f = M_b \tag{4}$$

The solution of the preceding equation for a model undergoing a steady-state oscillation at an amplitude, $\overline{\theta}_m$, is

$$\begin{aligned}
\theta_f &= \overline{\theta}_f \cos(\omega t) \\
\theta_s &= \overline{\theta}_s \cos(\omega t + \Gamma) = \overline{\theta}_s[\cos(\omega t)\cos\Gamma - \sin(\omega t)\sin\Gamma] \\
z &= -\overline{z}\cos(\omega t + \Gamma) = -\overline{z}[\cos(\omega t)\cos\Gamma - \sin(\omega t)\sin\Gamma] \\
M_b &= \overline{M}_b \cos(\omega t + \gamma) = \overline{M}_b[\cos(\omega t)\cos\gamma - \sin(\omega t)\sin\gamma]
\end{aligned} \tag{5}$$

If the frequency of oscillation is not near the natural frequency of the sting ($\omega_{n_s} > 1.5\omega$) and the system is rigidly mounted, the phase angle, Γ, will be near zero or 180 deg, depending on the variation of normal force with θ_m. The phase angle is measured by the resolvers (divide Output 4 by 5, Fig. 3b) to verify this premise. Substituting Eq. (5) with sin Γ = 0 (cos Γ terms are left primarily to obtain the correct sign) into Eq. (4) and solving for the aerodynamic moments gives

$$M_\alpha = M_{\theta_f}\left[\left(\frac{\omega}{\omega_{n_f}}\right)^2 - 1\right] + \left(M_{\theta_f}\frac{\bar{\theta}_s \cos\Gamma}{\bar{\theta}_f} - \delta M_{\theta_f} - \frac{\bar{M}_b}{\bar{\theta}_f}\cos\gamma - Wx_{cg}\omega^2\frac{\bar{z}\cos\Gamma}{\bar{\theta}_f}\right)\Bigg/\left(1 + \frac{\bar{\theta}_s\cos\Gamma}{\bar{\theta}_f}\right) \tag{6}$$

$$M_q + M_{\dot{\alpha}} = \left(-\frac{\bar{M}_b}{\omega\bar{\theta}_f}\sin\gamma + \frac{M_\alpha}{V_\infty\cos\alpha_M}\frac{\bar{z}\cos\Gamma}{\bar{\theta}_f} - M_{\dot{\theta}_f}\right)\Bigg/\left(1 + \frac{\bar{\theta}_s\cos\Gamma}{\bar{\theta}_f}\right) \tag{7}$$

where $-M_{\theta_f}/\omega_{n_f}^2$ has been substituted for I_y and the term

$\frac{\bar{z}}{\bar{\theta}_f}\frac{\omega^2}{V_\infty\cos\alpha_M} M_{\dot{\alpha}}$, which is very small, has been omitted in Eq. (6).

M_{θ_f} is determined during the balance calibration, and the model unbalance Wx_{cg}, can be obtained from the balance static outputs. The terms $\frac{\bar{M}_b}{\bar{\theta}_f}\cos\gamma$ and $\frac{\bar{M}_b}{\bar{\theta}_f}\sin\gamma$ can be obtained from the resolver Outputs 1, 2, and 3 (Fig. 3b), along with the balance calibration constants. $M_{\dot{\theta}_f}$ and ω_{n_f} can be determined by evaluating the system at vacuum conditions similar to that discussed in Ref. 1.

The ratio of the in-phase sting deflection amplitudes to the flexure amplitude can be determined from the moments measured by the cross flexures and the sting gages,

$$\frac{\bar{\theta}_s\cos\Gamma}{\bar{\theta}_f} = -M_{\theta_f}\left(\frac{\partial\theta_s}{\partial M_p}\right) + \left(\frac{\bar{M}_s\cos\Gamma}{\bar{\theta}_f}\right)\left(\frac{\partial\theta_s}{\partial M_s}\right)$$

$$\frac{\bar{z}\cos\Gamma}{\bar{\theta}_f} = M_{\theta_f}\left(\frac{\partial z}{\partial M_p}\right) - \left(\frac{\bar{M}_s\cos\Gamma}{\bar{\theta}_f}\right)\left(\frac{\partial z}{\partial M_s}\right)$$

where the partial derivatives are determined from sting calibration and $\left[(\bar{M}_s/\bar{\theta}_f)\cos\Gamma\right]$ is determined from resolver Outputs 1 and 5

(Fig. 3b), along with calibration constants. If the sting is not instrumented and static-force data are available $\left[(\overline{M}_S/\bar{\theta}_f) \cos \Gamma\right]$ can be determined from the force equation of motion. The aerodynamic moments can be expressed in dimensionless form as:

$$C_{m_\alpha} = M_\alpha / q_\infty Ac$$

$$C_{m_q} + C_{m_{\dot{\alpha}}} = \frac{(M_q + M_{\dot{\alpha}})(2V_\infty)}{q_\infty Ac^2}$$

The preceding analysis has been written for a model oscillating in pitch, but the mechanism can be rolled 90 deg with respect to the model and used to determine the yaw derivatives. The preceding equations also apply for yaw, although the oscillatory sting deflections are usually considerably smaller. For yaw, the pitch coefficients, C_{m_α} and $C_{m_q} + C_{m_{\dot{\alpha}}}$, are replaced by $-C_{n_\beta} \cos \alpha_M$ and $C_{n_r} - C_{n_{\dot{\beta}}} \cos \alpha_M$, respectively. The $\cos \alpha_M$ term is a result of expressing the coefficients in the body-axis system.

In the preceding analysis the balance input torque, M_b, signal has been assumed to be the first harmonic of the oscillation frequency, ω. Because of nonlinear aerodynamics, tunnel noise, flow perturbations, etc., the signal is often composed of higher and lower harmonics. However, the resolver system (Fig. 3b) eliminates the higher harmonics, and the lower harmonics can be eliminated by averaging the data over a sufficiently long interval.

3.2 CALIBRATION AND BENCH TESTS

The cross-flexure stiffness, M_{θ_f}, and calibration constant, K_o, were determined by applying known moments and measuring the deflection across the flexure and the strain-gage output. The sting deflection constants, $\partial\theta_S/\partial M_p$, $\partial\theta_S/\partial M_S$, $\partial z/\partial M_p$ and $\partial z/\partial M_S$, and calibration constant, K_S, were obtained by applying known loads at different axial locations. The moment-beam calibration constant, K_1, was determined at assembly by applying steady loads (various levels up to the beam capacity) with the motor and measuring the outputs of the moment beam and the flexures. The applied moment is known from the flexure output.

Bench tests were conducted with the system to determine its capability for measuring the damping moment. A two-arm magnetic calibrator, developed at the VKF, was used to produce known damping moments. A signal coil, input coil, and feedback loop were used in the calibrator which could produce both stable and unstable moments. The tests were conducted with the calibration body balanced about the pivot axis and also with a large unbalance. This unbalance caused oscillations of the sting when conventionally mounted, but the sting could also be rigidly supported during the bench tests to eliminate these oscillations.

3.3 WIND TUNNEL TESTS

Verification tests were conducted at Mach numbers of 2.5, 3.0, 3.5, and 4.0, at a Reynolds number of 4×10^6, based on the mean aerodynamic chord, and at angles of attack from -4.7 to 11.5 deg. A summary of test conditions is presented in Table I. Before testing, the models were balanced about the pivot axis within 0.1 in.-lb, and the still air contributions were measured (Ref. 1). The data were obtained primarily at an oscillation amplitude of ±0.9 deg and at the natural frequency (γ = 90 deg); however, some data were obtained at other conditions to check the instrumentation. Wind-off data were obtained before and after testing each model to evaluate $M_{\dot{\theta}_f}$ and ω_{n_f}.

TABLE I
SUMMARY OF TEST CONDITIONS

Configuration*	Mach No.	p_o, psia	T_o, °R	q_∞, lb/ft^2	V_∞, ft/sec	$Re_{\infty,c} \times 10^{-6}$	α_M, deg
2	2.50	24	560	885	1933	3.98	-3.5 to 2.5
3	2.50	24	560	885	1933	3.98	-3.0 to 9.9
1	3.01	32	562	784	2085	4.05	-2.7 to 2.8
2	3.01	32	↓	784	2085	4.05	-4.7 to 4.8
3	3.01	32	↓	784	2085	4.05	-3.4 to 11.3
1	3.50	42	↓	680	2189	4.11	-3.2 to 3.3
2	3.50	42	↓	680	2189	4.11	-4.5 to 4.5
3	3.50	42	↓	680	2189	4.11	-3.8 to 11.5
1	4.02	55	583	574	2313	3.88	-3.5 to 3.7
2	4.02	55	583	574	2313	3.88	-4.0 to 5.5
3	4.02	55	583	574	2313	3.88	-3.7 to 11.3

*Configuration 1: AGARD Model B Body Alone
2: AGARD Model B
3: AGARD Model C

SECTION IV
PRECISION OF MEASUREMENTS

The uncertainty in the measurements is a function of the precision of the calibration and sting deflection constants, instrumentation accuracy, repeatability of the flexure characteristics (wind-off data), and the phase relations. The uncertainties in the dynamic data as a result of the propagation of these errors (Ref. 4) can be written:

$$\Delta M_\alpha = \left\{(0.005\, M_\alpha)^2 + M_{\theta_f}{}^2\left[\left(\frac{2\Delta\omega_{n_f}}{\omega_{n_f}}\right)^2 + \left(0.03\,\frac{\bar{\theta}_s}{\bar{\theta}_f}\right)^2\right] + \left[\bar{W}x_{cg}\omega^2\left(\frac{\bar{z}}{\bar{\theta}_f}\right)(0.03)\right]^2 + \left[(0.1)\,\delta M_{\theta_f}\right]^2\right\}^{1/2}$$

$$\Delta(M_q + M_{\dot{\alpha}}) = \left\{\left(\frac{\bar{M}_b}{\bar{\theta}_f\omega}\sin\gamma\right)^2\left[\left(\frac{0.009}{\tan\gamma}\right)^2 + (0.0148)^2\right] + \left(\frac{M_\alpha}{V_\infty}\,\frac{\bar{z}}{\bar{\theta}_f}\right)^2\left[\left(\frac{\Delta M_\alpha}{M_\alpha}\right)^2 + (0.03)^2\right]\right.$$

$$\left. + \left[\Delta\left(M_{\dot{\theta}_f}\right)\right]^2 + \left(0.01\, M_{\dot{\theta}_f}\right)^2\right\}^{1/2}$$

where the following uncertainties have been used:

$$\Delta M_{\theta_f}/M_{\theta_f} = 0.005$$

$$\Delta(\bar{M}_b)/\bar{M}_b = 0.01$$

$$\Delta(\bar{\theta}_f)/\bar{\theta}_f = 0.01$$

$$\Delta(\bar{z})/\bar{z} = 0.03$$

$$\Delta(\bar{\theta}_s)/\bar{\theta}_s = 0.03$$

$$\Delta\gamma = 0.009 \text{ radians } (0.5 \text{ deg})$$

$$\Delta\left(\delta M_{\theta_f}\right)/\left(\delta M_{\theta_f}\right) = 0.1$$

It is apparent that the most accurate damping data are obtained at the resonant frequency (γ = 90 deg), but the precision is not significantly affected if $30 < \gamma < 150$ deg. The uncertainty in measuring M_q at γ = 90 deg during the bench tests was the larger of 1.5 percent of the value measured or 0.001 ft-lb-sec/radian and was 5.2 percent of the value measured when γ = 5 or 175 deg.

Measurement of the tunnel model-support system attitude in pitch is precise within ±0.05 deg based on repeat calibrations. Model attitude corrections were made for balance and sting deflections under air load, and the precision of the final model mean angle of attack, α_M, is estimated to be ±0.07 deg. The uncertainty in the static pitching moment is determined from a statistical analysis of the data obtained during calibration where loads were applied to simulate the range of model loads anticipated for the test.

The preceding uncertainties were combined with uncertainties in the tunnel parameters to obtain the probable error in the aerodynamic coefficients. The maximum uncertainties are:

M_∞	$\Delta(M_\infty)$	$Re_{\infty,c} \times 10^{-6}$	$\Delta(Re_{\infty,c} \times 10^{-6})$	$\frac{\Delta(C_{m_q} + C_{m_{\dot\alpha}})}{C_{m_q} + C_{m_{\dot\alpha}}}$	$\Delta(C_{m_\alpha})$	$\Delta(C_m)$
2.50	0.004	3.98	0.024	0.020	0.0075	0.00045
3.01	0.006	4.05	0.024	0.020	0.0085	0.00050
3.50	0.005	4.11	0.022	0.020	0.0098	0.00058
4.02	0.010 σ .020 2σ	3.88	0.032	0.022	0.0116	0.00069

SECTION V
RESULTS AND DISCUSSION

The results obtained in the bench tests are presented in Fig. 6. The damping measurement (M_q) shows excellent agreement with the calibrator input ($M_{q_{mag}}$) over a large range of magnitudes (Fig. 6a) and phase angles (Fig. 6b). The uncertainty in the calibrator is 2 percent of the input value. Figure 6a also shows the effect of the sting oscillation (caused by an unbalance) on the damping measurement and indicates that good data can be obtained if the sting oscillations are included in the data reduction. For the bench tests there were no corrections because of the z movement which only affects aerodynamic measurements (see Equation (7), Section 3.1). The legend of Fig. 6 shows that the natural frequency (ω_{n_f}) of the model-flexure system can be determined very accurately if the sting oscillations are considered (53.92 as compared with 53.45) but is considerably in error if the sting oscillation corrections are omitted (49.72). The model moment of inertia, I_y, which was constant for all three unbalanced cases (Wx_{cg} = 0.328) would have been calculated erroneously if the sting oscillation corrections had not been applied.

Sym	Wx_{cg}, slug-ft^2	I_y, slug-ft^2	ω_{n_f}, rad/sec	Sting	
○	0	0.312	54.85	Rigid	
□	0.233	0.328	53.45	Rigid	
□	0.233	0.328	49.72	Oscillating	(Sting Bending Effect Not Included in Data Reduction)
■	0.233	0.328	53.92	Oscillating	(Sting Bending Effect Included in Data Reduction)

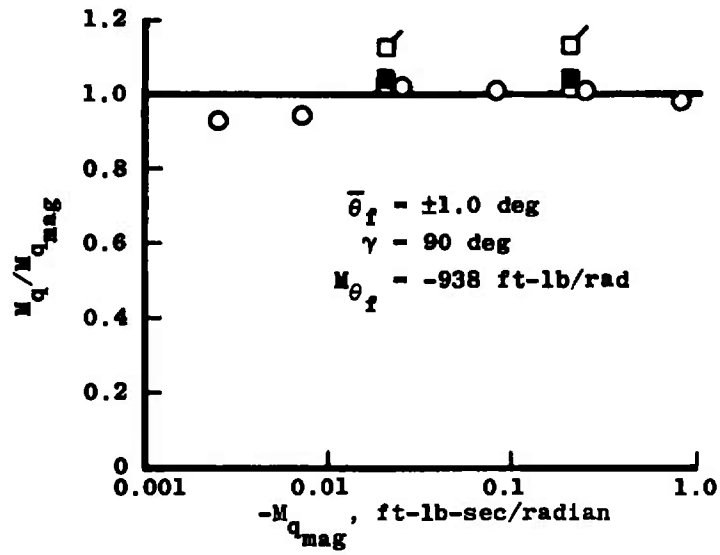

a. Variation with Damping Magnitude

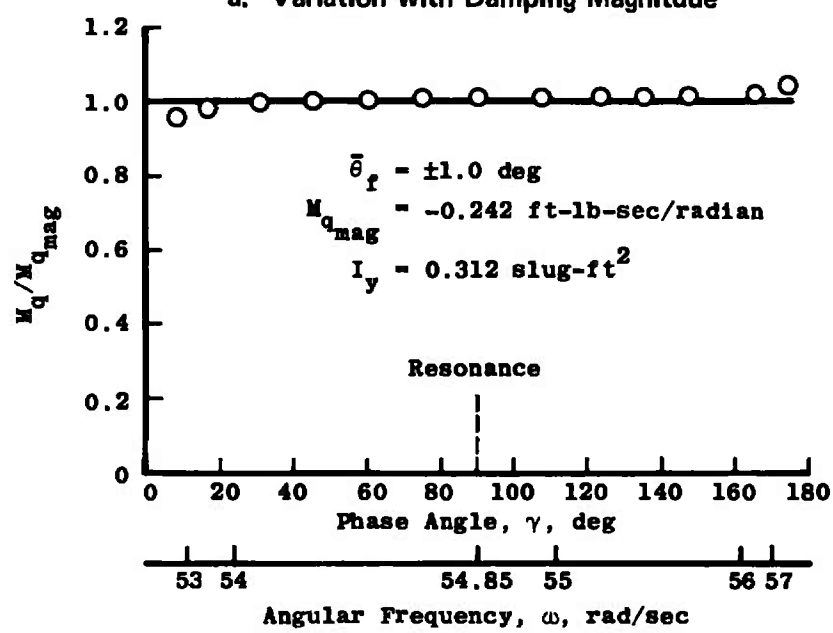

b. Variation with Phase Angle and Frequency

Fig. 6 Comparison of Pitch-Damping Measurement to Magnetic Calibrator Input

The stability derivatives obtained in the wind tunnel verification tests for the AGARD calibration Model C at $M_\infty = 2.5$ are presented in Fig. 7 to show the effect of sting oscillations on the data. Omitting the sting oscillations from the data reduction results in measurements which indicate too much dynamic stability and too little static stability. The static stability derivative, C_{m_α}, obtained from the slope of the C_m versus α_M measurements is also presented in Fig. 7 and is in excellent agreement with the oscillatory data which have been corrected for sting oscillations.

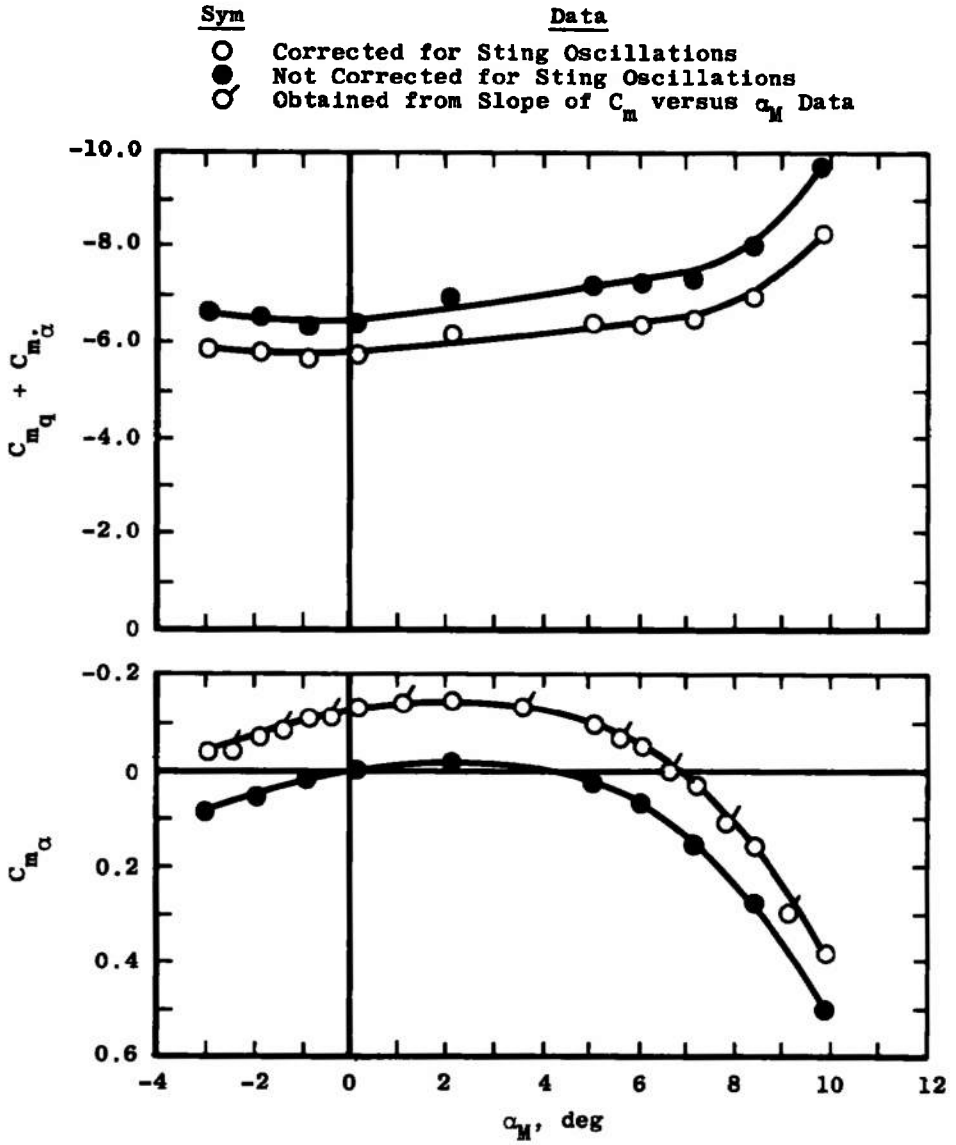

Fig. 7 Effect of Sting Oscillations on the Pitch Stability Derivatives of Model C at Mach 2.5

The experimentally measured dynamic and static stability derivatives at zero angle of attack are presented in Fig. 8 as a function of Mach number. The dynamic stability of Model C decreases slightly with increasing Mach number, whereas the dynamic stability of Model B and Model B body alone is practically invariant with Mach number. Estimates of $C_{m_q} + C_{m_{\dot{\alpha}}}$ for Model B were obtained from Refs. 5 (wing) and 6 (body) and are in good agreement with the present data. The trend of the static stability derivative, C_{m_α}, with Mach number varies considerably with the model configuration. The largest gradient of C_{m_α} with M_∞ is obtained with Model C which changes from stable to unstable at $M_\infty \approx 2.8$. The data obtained from the slope of the C_m versus α_M are presented and are in excellent agreement with the oscillatory data.

All of the data obtained in the wind tunnel tests on the AGARD calibration Models B and C and Model B body are presented in Fig. 9 as a function of angle of attack at Mach numbers of 2.5, 3.0, 3.5, and 4.0. All models were dynamically stable, and the dynamic stability of Model C generally increased as $|\alpha|$ increased, whereas the dynamic stability of Model B and Model B body decreased slightly with $|\alpha|$. Addition of the tail assembly (Model C compared with Model B) increased the dynamic stability considerably, but the wings caused only a slight increase in the stability (Model B compared with Model B body alone). Theoretical estimates obtained from Ref. 5 indicate the wing damping to be small ($C_{m_q} + C_{m_{\dot{\alpha}}} = -0.23$ at $M_\infty = 2.5$, -0.14 at $M_\infty = 4.0$).

The models were shown to be statically unstable at all test conditions except Model C at $M_\infty = 2.5$. The static stability (C_{m_α}) of Model B and Model B body alone is practically invariant with angle of attack, but the static stability of Model C has some very nonlinear characteristics which vary with Mach number. The static data from Ref. 7 are also shown in Figs. 9a, b, and d and are in good agreement with the present results.

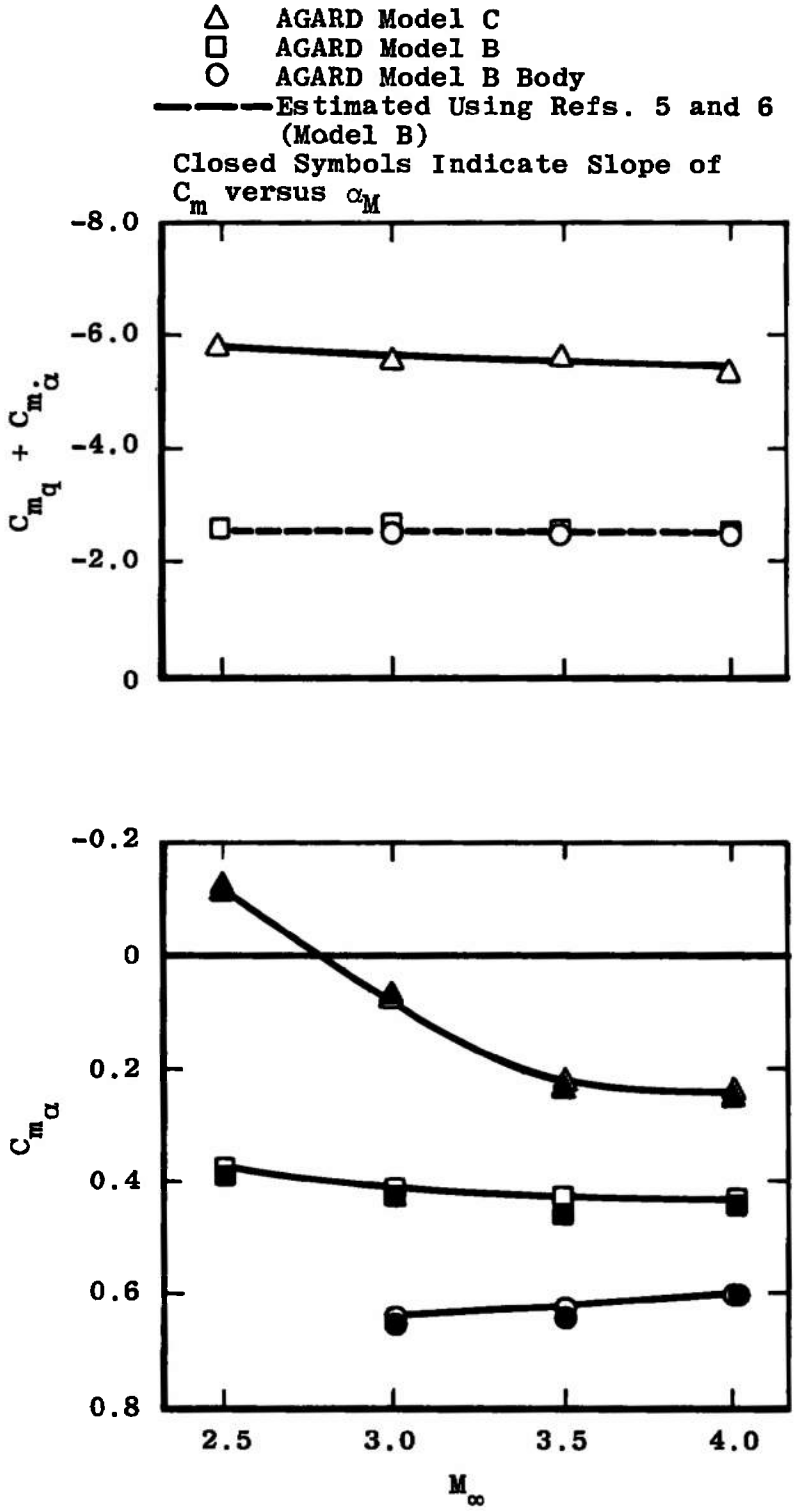

Fig. 8 Variation of the Pitch Stability Derivatives at α_M = 0 with Mach Number

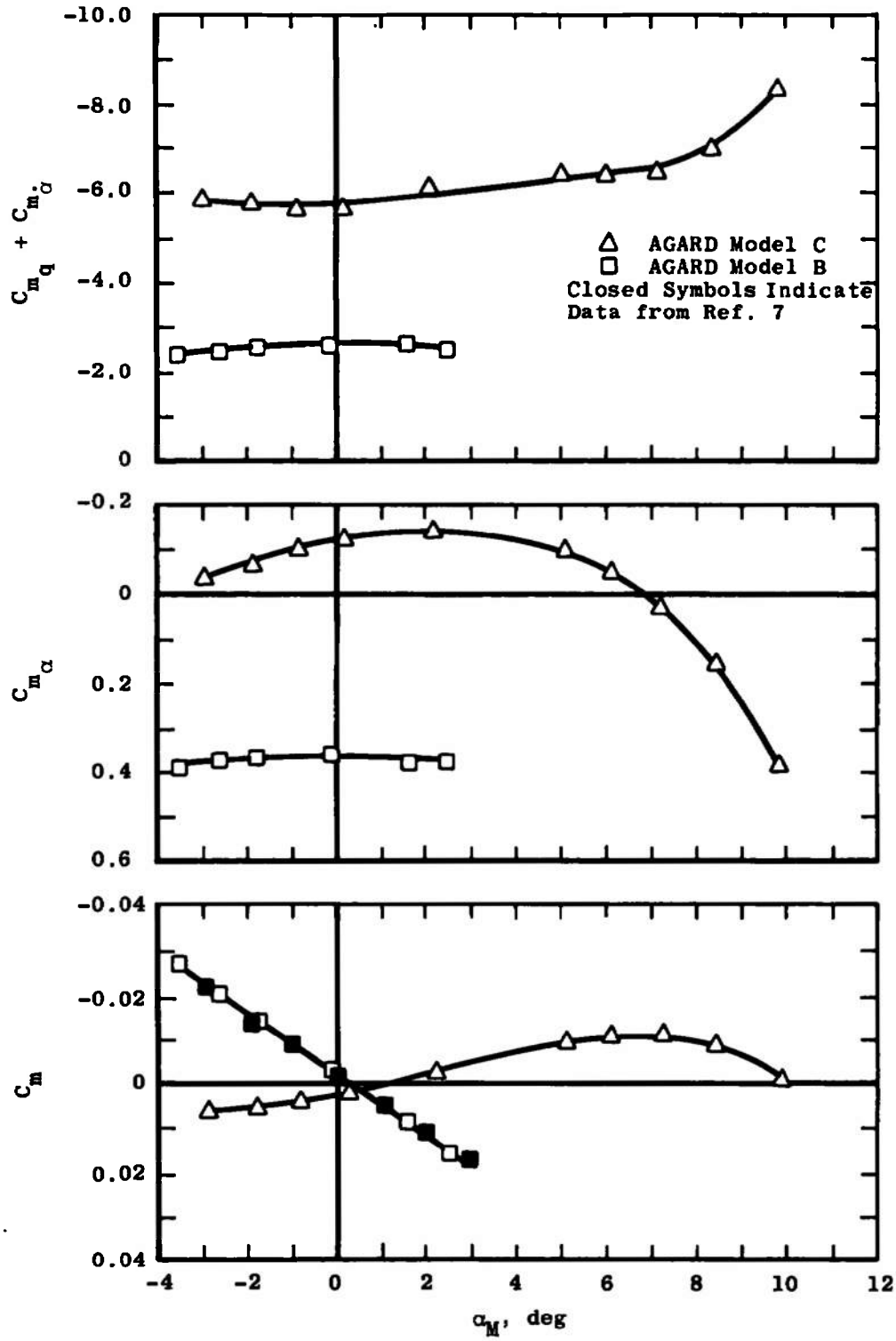

a. $M_\infty = 2.5$

Fig. 9 Variation of the Pitch Stability Characteristics with Angle of Attack

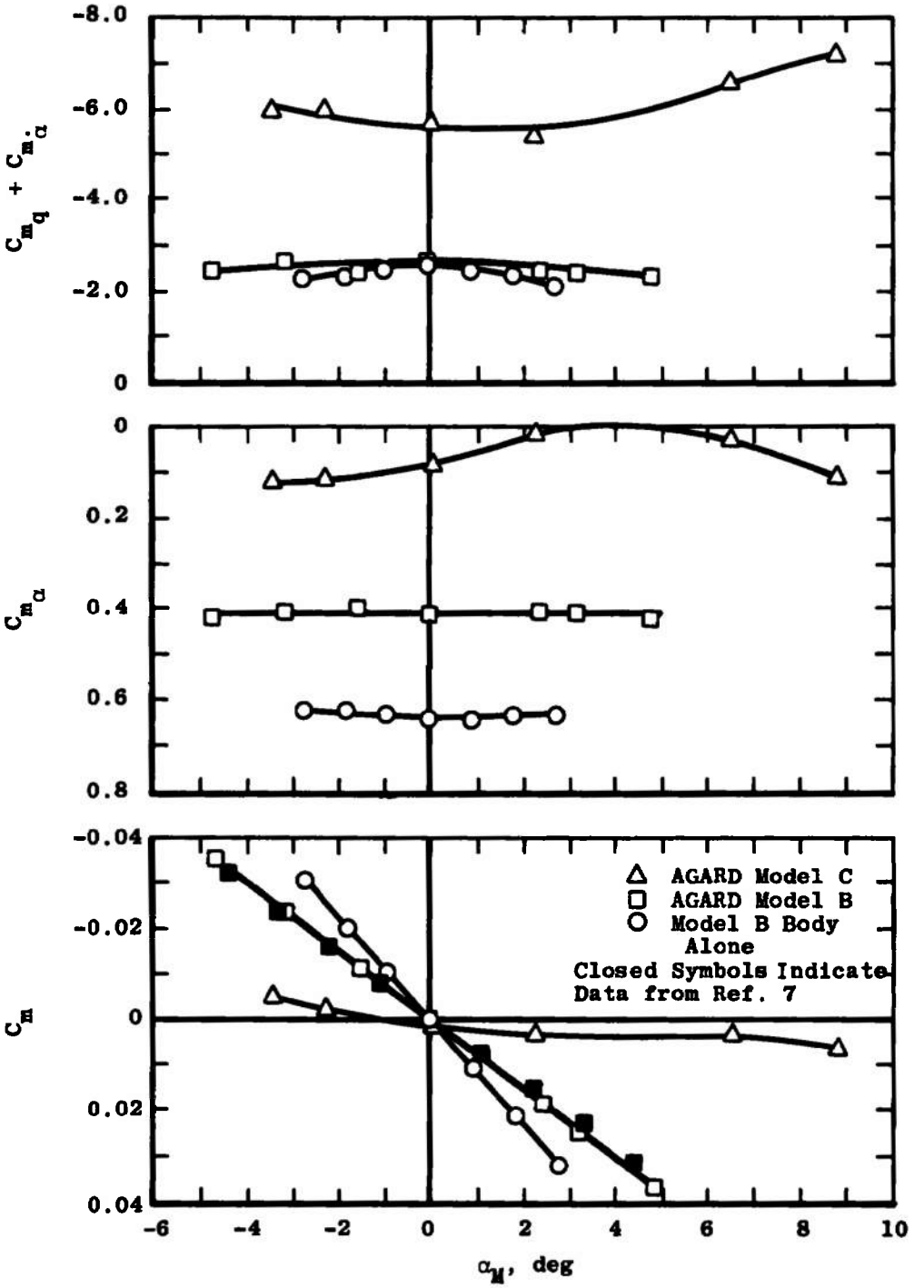

b. $M_\infty = 3.0$

Fig. 9 Continued

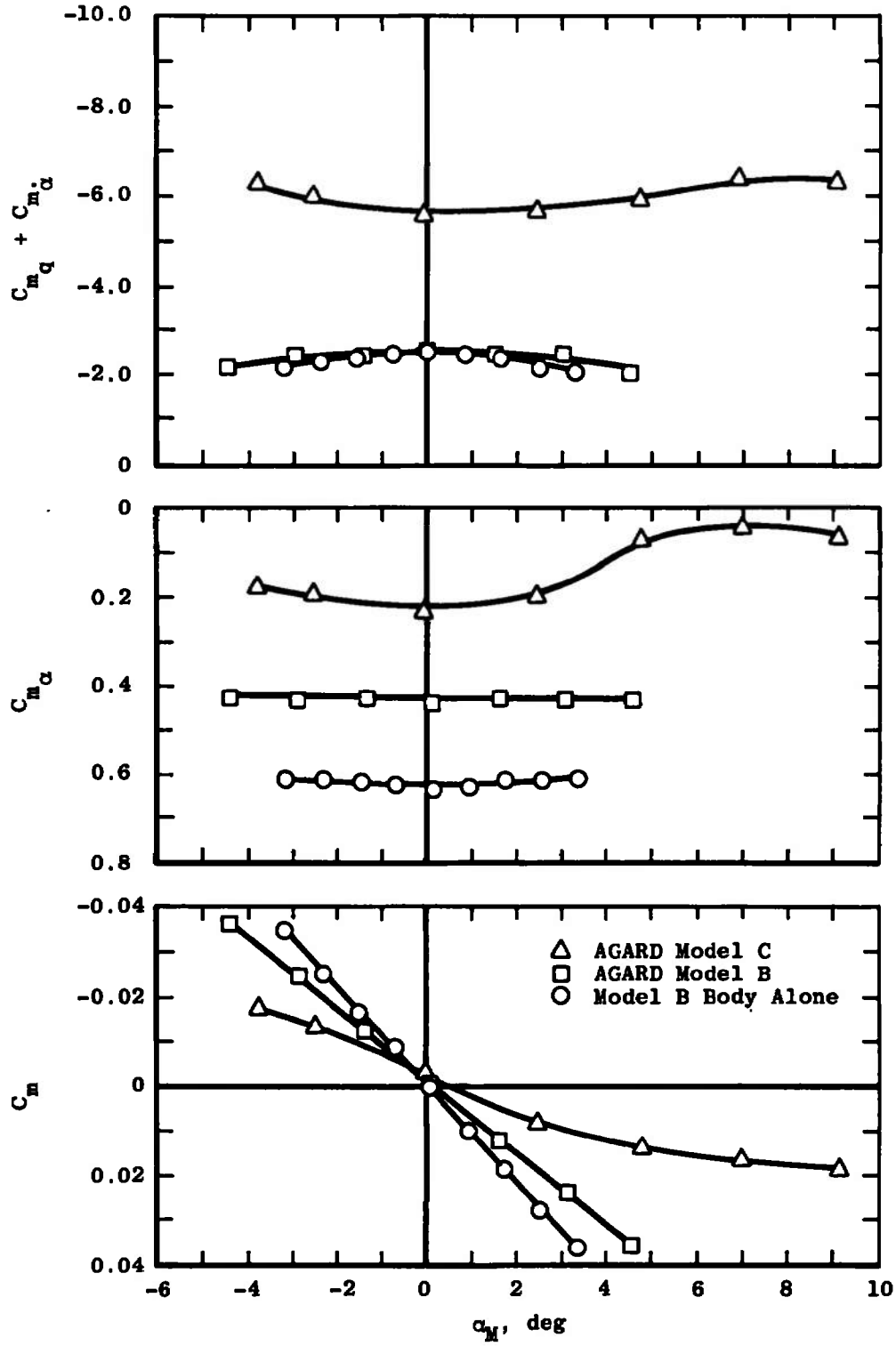

c. $M_\infty = 3.5$

Fig. 9 Continued

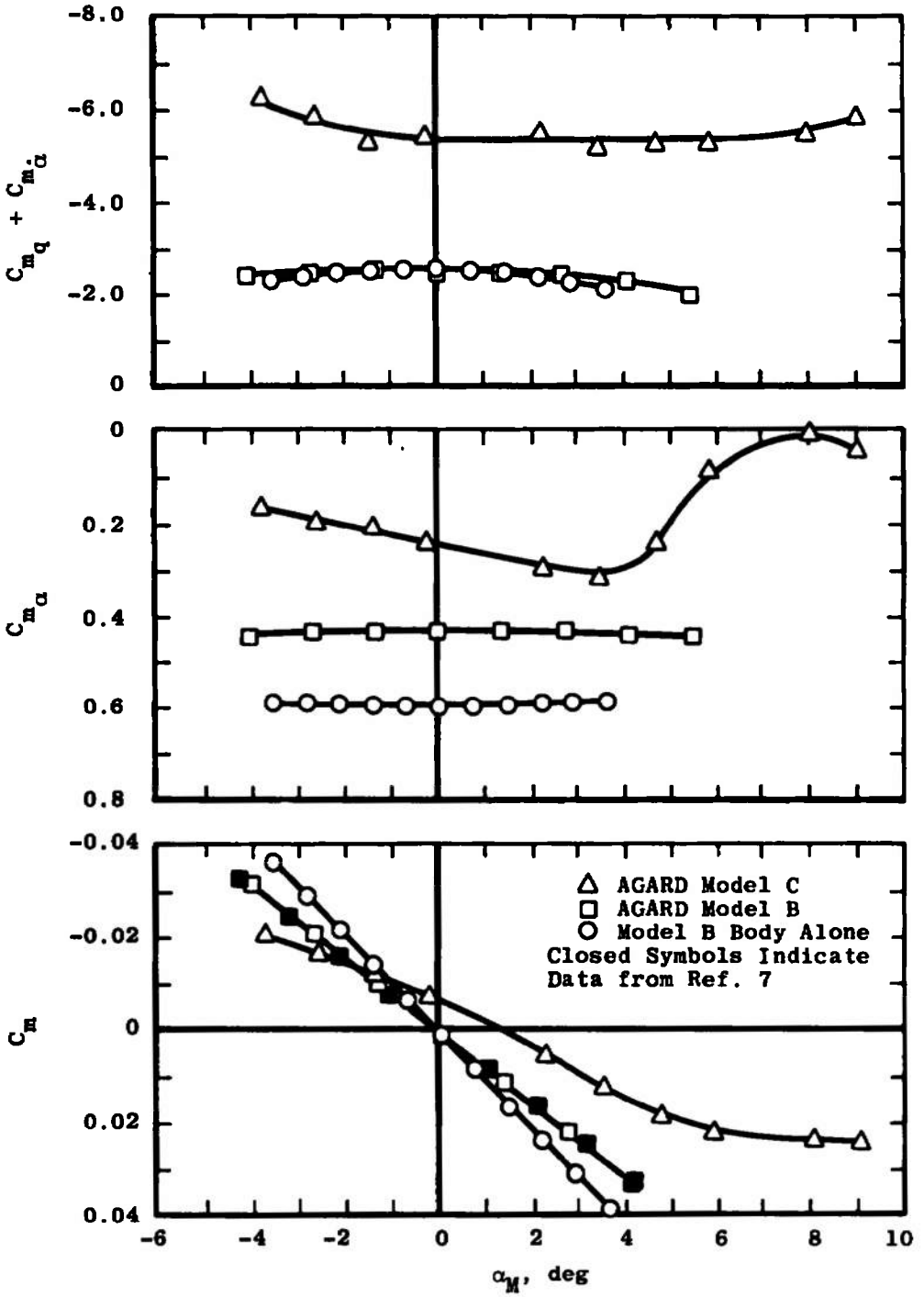

d. $M_\infty = 4.0$

Fig. 9 Concluded

SECTION VI
CONCLUSIONS

A forced-oscillation test mechanism for measuring the dynamic stability derivatives in pitch or yaw on lifting configurations was developed. Bench and wind tunnel tests on AGARD Calibration Models B and C and Model B body alone were conducted to evaluate and verify the mechanism design and performance. Conclusions based on the results of these tests are as follows:

1. The dynamic stability derivatives and slope of the pitching-moment curve obtained from oscillatory data can be measured precisely by the mechanism providing the effects of sting oscillations are included in the data reduction equations.
2. Omitting the sting oscillations from the data reduction causes considerable error in the data.
3. The results of the wind tunnel tests are in good agreement with previous experimental data and theoretical estimates.

REFERENCES

1. Schueler, C. J., Ward, L. K., and Hodapp, A. E., Jr. "Techniques for Measurements of Dynamic Stability Derivatives in Ground Test Facilities." AGARDograph 121 (AD669227), October 1967.
2. Burt, G. E. "A Description of a Forced-Oscillation Test Mechanism for Measuring Dynamic-Stability Derivatives in Roll." AEDC-TR-73-49.
3. Wittrick, W. H. "The Theory of Symmetrical Crossed Flexure Pivots." Council for Scientific and Industrial Research, Dept. of Aeronautics Report SM. 108, Melbourne, Australia, January 1948.
4. Beers, Yardley. Introduction to the Theory of Error. Addison-Wesley Publishing Co., Inc., Reading, Mass., 1957, pp. 26-36.

5. Henderson, Arthur, Jr. "Pitching-Moment Derivatives C_{m_q} and $C_{m_{\dot{\alpha}}}$ at Supersonic Speeds for Slender-Delta-Wing and Slender-Body Combination and Approximate Solutions for Broad-Delta-Wing and Slender-Body Combination." NACA TN 2553, December 1951.

6. Murphy, C. H. and Schmidt, L. E. "The Effect of Length on the Aerodynamic Characteristics of Bodies of Revolution in Supersonic Flight." BRL Report 876, August 1953.

7. Coats, Jack D. "Force Tests of an AGARD Calibration Model B at M = 2.5 to 6.0." AEDC-TN-60-182, October 1960.

UNCLASSIFIED

Security Classification

DOCUMENT CONTROL DATA - R & D

(Security classification of title, body of abstract and indexing annotation must be entered when the overall report is classified)

1 ORIGINATING ACTIVITY (Corporate author)	2a. REPORT SECURITY CLASSIFICATION
Arnold Engineering Development Center Arnold Air Force Station, Tennessee 37389	UNCLASSIFIED
	2b. GROUP N/A

3 REPORT TITLE

A DESCRIPTION OF A PITCH/YAW DYNAMIC STABILITY, FORCED-OSCILLATION TEST MECHANISM FOR TESTING LIFTING CONFIGURATIONS

4 DESCRIPTIVE NOTES (Type of report and inclusive dates)

Final Report - April 13, 1972

5 AUTHOR(S) (First name, middle initial, last name)

G. E. Burt, ARO, Inc.

6 REPORT DATE	7a. TOTAL NO OF PAGES	7b. NO. OF REFS
June 1973	35	7

8a. CONTRACT OR GRANT NO	9a. ORIGINATOR'S REPORT NUMBER(S)
b. PROJECT NO	AEDC-TR-73-60
c. Program Element 65808F	9b. OTHER REPORT NO(S) (Any other numbers that may be assigned this report)
d.	ARO-VKF-TR-73-16

10 DISTRIBUTION STATEMENT

Approved for public release; distribution unlimited.

11 SUPPLEMENTARY NOTES	12 SPONSORING MILITARY ACTIVITY
Available in DDC	Arnold Engineering Development Center, Air Force Systems Command Arnold Air Force Station, TN 37389

13 ABSTRACT A forced-oscillation test mechanism for measuring the dynamic stability derivatives in pitch or yaw on lifting configurations has been developed at AEDC-VKF. The mechanism will support models with a combined loading up to 1200-lb normal force and 300-lb axial force. Wind tunnel verification tests were conducted on AGARD Calibration Models B and C and Model B body alone at Mach numbers of 2.5, 3.0, 3.5, and 4.0 and at angles of attack from -4.5 to 11.5 deg. A description of the apparatus, testing technique, data reduction equations (including effects of sting bending), and the results from the laboratory bench and wind tunnel tests are included. The results of these tests were in good agreement with previous experimental data and theory.

DD FORM 1 NOV 65 1473

UNCLASSIFIED

Security Classification

14. KEY WORDS	LINK A		LINK B		LINK C	
	ROLE	WT	ROLE	WT	ROLE	WT
description						
pitch/yaw						
dynamic stability						
oscillation (forced)						
test equipment						
lifting bodies						
configurations						
Mach numbers						

AFSC
Arnold AFS Tenn